JOURNAL OF MATERIALS SCIENCE 31 (1996) 673–677

A thermoanalytical study of oxidation of TiC by simultaneous TGA–DTA–MS analysis

S. SHIMADA
Department of Applied Chemistry, Faculty of Engineering, Hokkaido University, Sapporo 060, Japan

The oxidation of TiC powders was non-isothermally carried out by heating up to 900 °C at a rate of 5 °C min^{-1} and at an oxygen pressure of 2–60 kPa, using a simultaneous thermogravimetric analysis–differential thermal analysis–mass spectroscopy (TGA–DTA–MS) apparatus. It was found that oxidation was divided into four stages, I to IV. Stage I, covering the oxidation fraction, α, 0–20%, was probably due to formation of oxycarbide (TiC_xO_{1-x}, $0 < x < 0.5$) with slight heat and CO_2 evolution. Oxidation in stages II and III at 20–60% was affected by oxygen pressure; the higher pressure giving rise to very sharp exothermic and CO_2 evolution peaks in stage II, which are correlated with the formation of anatase. Oxidation in stage III proceeded gradually with increasing rutile phase. The sample amount also exerted a similar effect on oxidation as the oxygen pressure.

1. Introduction

Many oxidation studies on TiC materials have been reported [1–6], most of which discuss the oxidation mechanism from a kinetic viewpoint. These summarize that oxidation of TiC parabolically proceeds under intermediate oxygen pressures (several to 100 kPa) and at temperatures of 600–800 °C, in contrast to linear oxidation at high temperatures and oxygen pressures.

The author has also reported the oxidation kinetics of TiC powder samples at relatively low temperatures of 350–500 °C, and demonstrated that oxidation is described by a one-dimensional diffusion equation, consisting of four steps, I–IV. [7] However, step I could not be clearly distinguished from step II from the kinetic curve, nor could the process occurring in this step be explained, because the step proceeded very rapidly when the sample was introduced into a hot zone kept at constant temperature. If the sample was non-isothermally oxidized at a constant heating rate, the reaction in step I could be followed because of the relatively slow oxidation. It was also noted that a sharp exothermic peak appeared on the DTA curve during oxidation, which was assumed to result from the crystallization of anatase, although no evidence was given in support of this. However, the sharp exothermic peak could be associated with rapid oxidation accompanying a large CO_2 evolution.

The author has reported the oxidation of ZrC [8, 9], HfC [10] and NbC [11, 12], using powder and single crystal samples. In the case of ZrC and HfC, it was revealed that much of the C component of the carbide is deposited in the oxide scale is an amorphous form in the course of oxidation, producing characteristically oxide layers [9]. On the other hand, the oxidation of NbC powders gave rise to a sudden release of CO_2 gas during oxidation, which was caused by explosive cracking of the NbC grains; such CO_2 evolution could be followed by MS. There have been few reports on the oxidation of carbide based on CO_2/CO analysis as well as DTA–TGA analysis. Thus, much attention has been paid to the oxidation behaviour of the C component of the carbide by the authors.

Thermal analysis of simultaneous TGA–DTA can provide useful information on the oxidation behaviour, as mentioned above, which cannot be obtained by conventional isothermal oxidation. If MS analysis is combined with the above, it can also serve as a powerful means for following CO_2 release. This study reported the oxidation behaviour of TiC powder at various oxygen pressures from a thermoanalytical viewpoint, using a simultaneous TGA–DTA–MS apparatus. The process in step I and the origin of the exothermic peak were clarified, and the effect of oxygen pressure and sample amount on oxidation was also examined.

2. Experimental procedure

The starting material was commercially available titanium carbide powders (purity 99.5%). The properties of the powder, such as major impurities, grain size and morphology, and surface area, have been reported previously [7]. Oxidation of TiC was followed to a temperature of 900 °C by simultaneous TGA–DTA–MS (TGA–DTA–MS 2000, MAC Science; VG Gas Analysis, Fisons Instrument) using a heating rate of 5 °C min^{-1} at an oxygen partial pressure of 2–60 KPa, achieved by mixing oxygen and argon gases. The sample, weighing from 2.7 to 19 mg, was placed in a Pt pan, 5 mm in diameter and 3 mm in height. The packed bed height when the 19 mg sample

0022–2461

was put in the pan was about 0.5 mm. During oxidation, weight gain and heat evolution, as well as CO_2 evolution, were simultaneously monitored as a function of temperature.

The phases present in the sample heated to a predetermined temperature were identified by X-ray powder diffraction (XRD). The lattice parameter of TiC was determined according to an internal standard method using Si powder. Morphologies of the oxidized TiC grains were observed by scanning electron microscopy (SEM).

The reacted fraction, α, was determined by dividing the measured weight gain by the theoretical one, which was calculated according to the equation (1)

$$TiC + 2O_2 = TiO_2 + CO_2 \qquad (1)$$

3. Results

Fig. 1 shows the TGA results of non-isothermal oxidation of TiC powder at an oxygen pressure of 2–60 kPa using a heating rate of 5 °C min^{-1}. Oxidation begins at about 300 °C, and finishes at 800 °C, irrespective of the oxygen pressure. It is seen that oxidation consists of four stages, I–IV. Stage I covers an α fraction range of 0–20%, proceeding relatively fast. Stages II and III occur in the range α = 20–60%, and occur at faster rates than stage I. Both stages cannot be separated from each other at the lower oxygen pressures of 2–10 kPa, above which stage II becomes noticeable with increasing pressure (shown by the arrow in Fig. 1) and proceeds very quickly. Increase of the α value owing to this rapid oxidation at 60 kPa reached more than 40%, apparently diminishing stage III. Stage IV proceeds above 60% at a slower rate than stages II and III.

Fig. 2 shows the DTA curves obtained simultaneously with TGA. It is seen that oxidation occurs exothermically, beginning around 300 °C and finishing around 800 °C, and that exothermic oxidation is divided into four temperature regions, 300–450, 450–470, 470–550 and > 550 °C, as shown by the dotted line on Fig. 2. These four regions correspond roughly to the four stages determined on the TGA curves. The second and third regions produce peaks A and B, respectively (Fig. 2C–E), and both peaks combine to become one peak, or overlap at 2–10 kPa, respectively (Fig. 2A, B). Peak A becomes sharper and shifts slightly to a lower temperature with increasing oxygen pressure, in contrast to a broadening and reducing peak B. The fourth exothermic peak occurs over a broad temperature range above 550 °C. It is noticed that a steep rise on the TGA curve around 460 °C corresponds to the sharp exothermic peak A.

CO_2 evolution during oxidation was followed simultaneously with the TGA–DTA measurement by S, as shown in Fig. 3. The evolution starts at 320 °C, at a temperature slightly higher than indicated by the TGA and DTA results, and finishes at 800–900 °C. Evolution occurs in four temperature regions: 320–440, 440–470, 470–550 and > 550 °C, in a very similar way to the heat evolution, as shown by the dotted lines in Fig. 3. In the second and third regions,

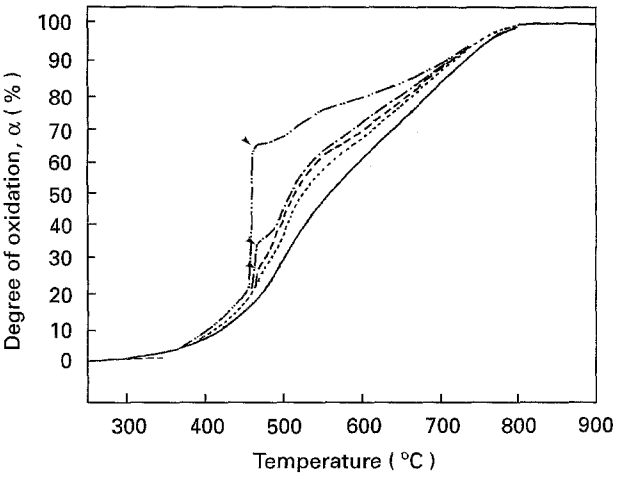

Figure 1 TGA curves in simultaneous TGA–DTA–MS for oxidation of TiC. Oxygen pressure (kPa) : (——) 2, (- - - -) 10, (– – –) 15, (–·–·–) 20, (–··–··–) 60 (heating rate, 5 °C min^{-1}; sample weight, ~11 mg).

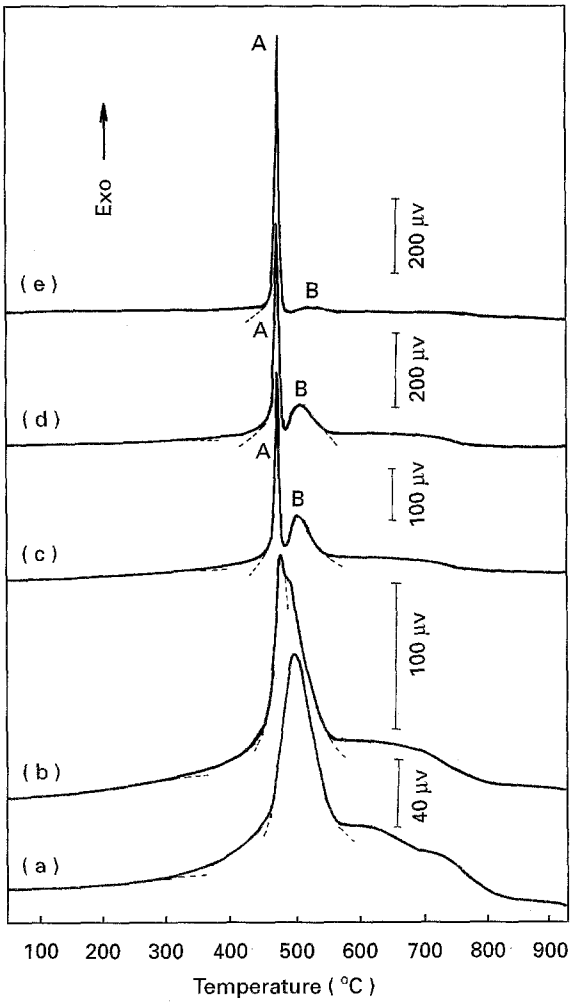

Figure 2 DTA curves in simultaneous TGA–DTA–MS for oxidation of TiC. Oxygen pressure (kPa) : (a) 2, (b) 10, (c) 15, (d) 20, and (e) 60 (heating rate, 5 °C min^{-1}; sample weight, ~11 mg).

peaks A′ and B′ appear (Fig. 3C, D), becoming overlapped at 2 and 10 kPa (Fig. 3A, B). A broad peak is recognized above 550 °C.

Fig. 4 shows the XRD patterns of the sample oxidized to various temperatures, i.e. to various α values, at 10 kPa. At the 9% fraction, only the TiC peaks are

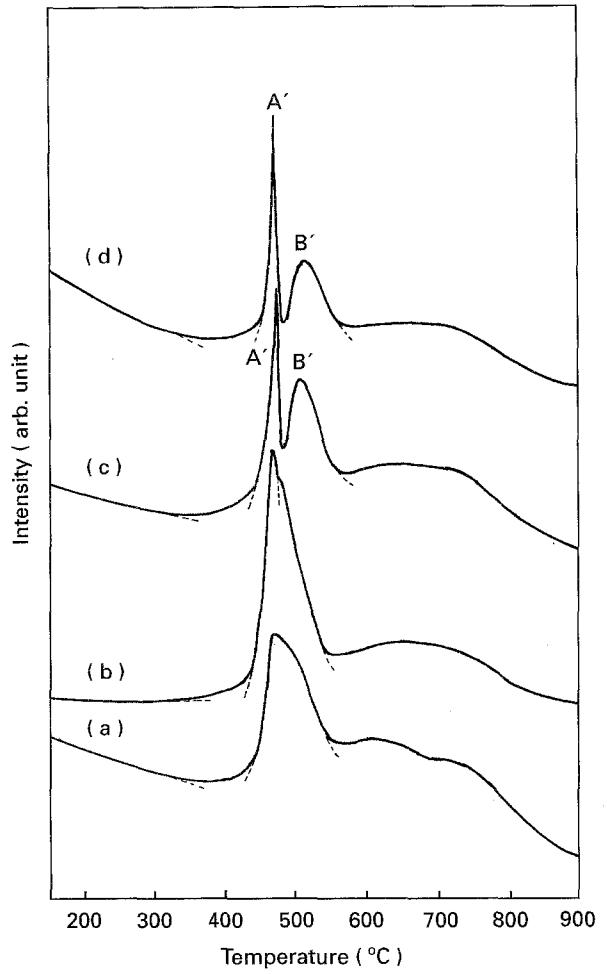

Figure 3 MS of CO_2 gas in simultaneous TGA–DTA–MS for oxidation of TiC. Oxygen pressure (kPa) : (a) 2, (b) 10, (c) 15, and (d) 20 (heating rate, 5 °C min^{-1}; sample weight, ~11 mg).

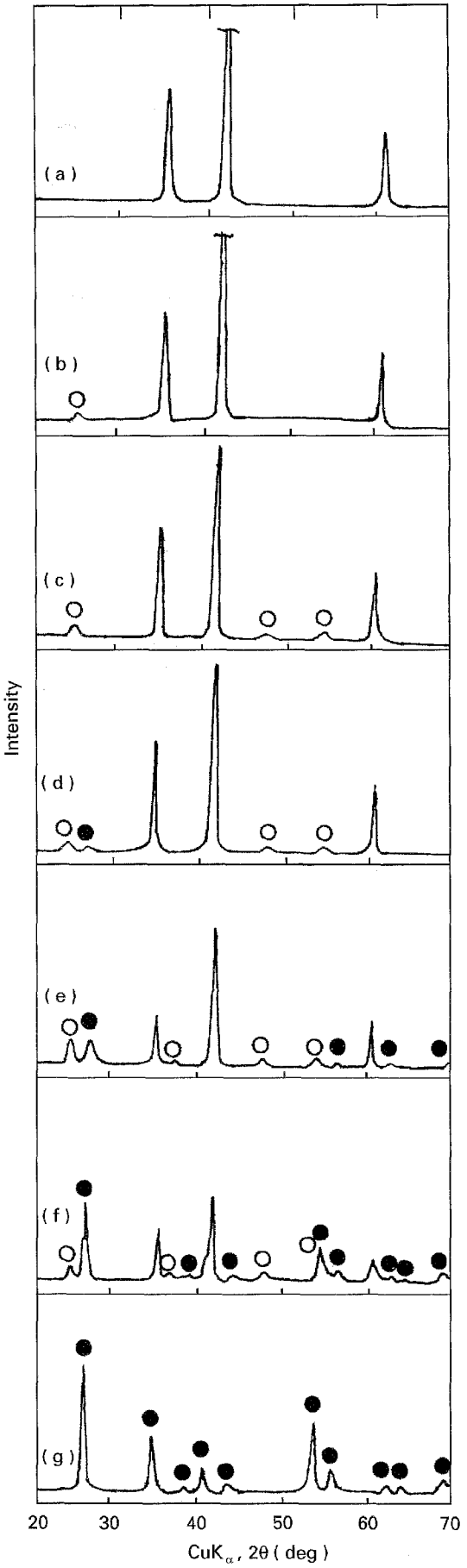

Figure 4 X-ray diffraction patterns of samples oxidized to various fractions at 10 kPa. Reacted fraction (%) : (a) 9, (b) 22, (c) 48, (d) 52, (e) 61, (f) 87, and (g) 100. (○) anatase, (●) rutile, (no mark) TiC.

seen (Fig. 4a). At 22%, a small broad peak of anatase (TiO_2) appears (Fig. 4b). The anatase peak hardly increases in spite of increasing oxidation fraction from 22 to 87%. A small formation of rutile is observed around 52%, which increases with increasing oxidation fraction (Fig. 4d–f). At the 100% fraction, only a rutile phase is formed (Fig. 4g).

The sample obtained for XRD was observed by SEM. No great change in the grains was observed at the 9–25% fractions. At 48%, small cracks are seen along the edges (Fig. 5a), which become greater with progressing oxidation, as exemplified by Fig. 5b. Some of the grains were completely broken into several pieces at the 100% fraction.

When the sample amount varied in the range 2.7–19 mg, peaks A and B on the DTA curve appeared as either separated sharp ones, or as overlapping or combined peaks. When an overlapping peak (Fig. 2b) is regarded as an intermediate peak between these separated and combined ones, two regions of occurrence of the latter two peaks are formed, depending on the pressure (Fig. 6). Only a combined peak was obtained for any sample weight at 2 kPa.

4. Discussion

It is clear from the weight and thermal changes (Figs 1 and 2) that oxidation begins at 300 °C and finishes at

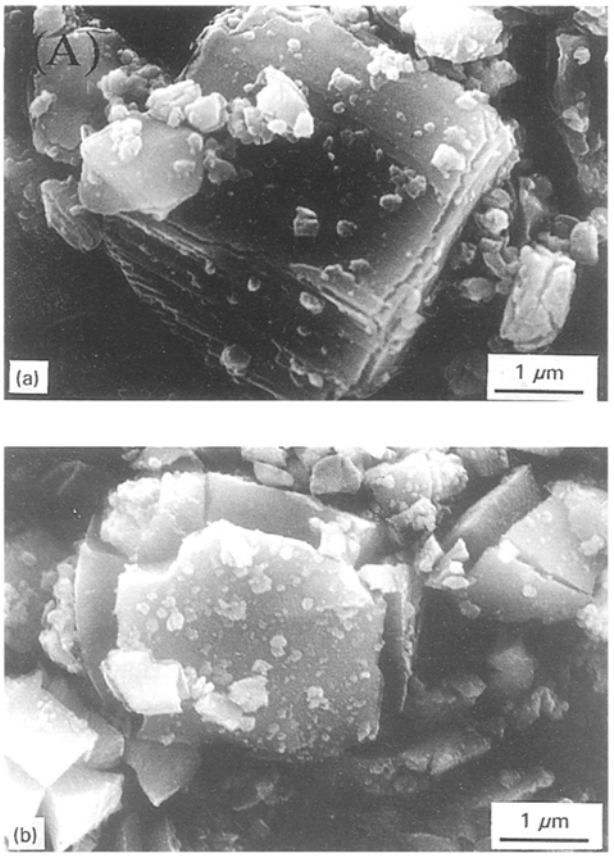

Figure 5 Scanning electron micrographs of the samples oxidized to (a) 48%, and (b) 87% at 10 kPa.

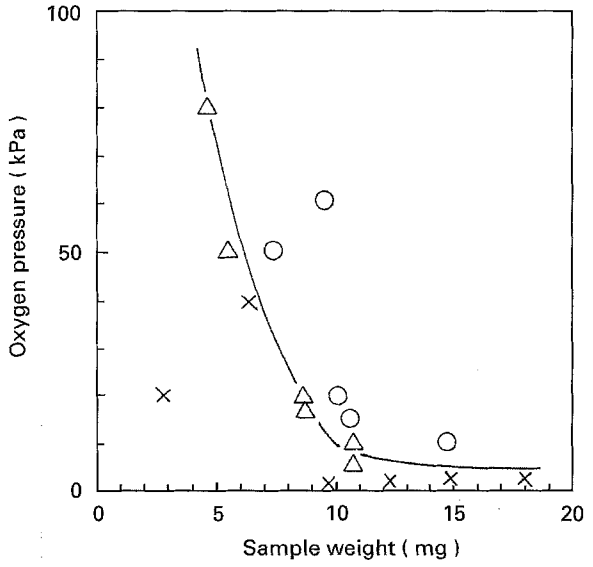

Figure 6 Diagram showing occurrence of (○) separated, (X) combined or (△) overlapping peak on the DTA curve with variation of oxygen pressure and sample weight.

800 °C. It was also found that oxidation is divided into four stages, I–IV; stage I covers the α fractions 0–20%, stages II and III 15–60% and stage IV the fractions above 60%. At higher pressures than 15 kPa, the fraction of stage II extends at the expense of stage III. Previous isothermal oxidation demonstrated that oxidation consists of four steps, I–IV; step I covered a fraction range below 10%, but reached a fraction more than 20% at the higher pressure of 16 kPa; step II, a range between 10 and 33%; step III, ranges between 10 and 33% and 45 and 50%; and step IV, a range above 45%. It is understood that the four stages obtained from the TGA–DTA results are in fairly good agreement with the four steps recognized by isothermal oxidation. Thus, stage I in non-isothermal oxidation corresponds to step I in the isothermal oxidation.

It is recognized that atomic oxygen can be substituted for the carbon present in the interstitial vacancies of the TiC lattice to form oxycarbide, TiC_xO_{1-x} ($x < 0.5$), the lattice parameter being reduced. The lattice parameter, a_0, of TiC in the oxidized sample was measured (Fig. 7), showing that a_0 decreases at the 4% fraction, then keeps almost constant. This result implies that at the beginning of oxidation (stage I), atomic oxygen is substituted for the carbon present in the TiC lattice to form oxycarbide, which continues to exist after stage I. The weight increase corresponding to $1-x = 0.5$ substitution equals 10%. In this stage, only the TiC peaks were detected by XRD. The previous electron diffraction result indicated that the sample oxidized to 6% contained titanium suboxides, such as TiO, Ti_3O_5 or Ti_4O_9. Thus, it is assumed that the slow rate of stage I was due to the formation of oxycarbide, followed by titanium suboxides, which produced the slight heat and CO_2 gas evolved. This stage was slightly enhanced with increasing oxygen pressure.

Oxidation was greatly accelerated in stage II. At pressures of 2 and 10 kPa, oxidation proceeded with a smooth rise of the α fraction (Fig. 1), accompanying either an overlapping or combined exothermic peak (Fig. 2A, B). At a pressure higher than 15 kPa, a steep rise of the α fraction was observed, the extent of which increased with increasing pressure; the pressure at 60 kPa raised the fraction to 60% (Fig. 2C–E). Both the overlapping heat and CO_2 evolution peaks were split into two peaks, A/B and A′/B′, corresponding to stages II and III, respectively, with increasing oxygen pressure. It is stressed that heat and CO_2 evolution showed one to one correspondence at each pressure. It was found that at 10 kPa, anatase had already formed at 22% fraction and slightly increased at 48% (Fig. 4), at which the high angle reflection lines of anatase appeared. Thus, oxidation in stage II must involve the formation of anatase, which accelerates oxidation at a higher oxygen pressure than 15 kPa. It is likely that consecutive reaction of TiC $\rightarrow TiC_xO_{1-x} \rightarrow$ titanium suboxide $\rightarrow$ anatase occurs, accompanying the large evolution of heat and CO_2 gas.

Stage III became apparent at α fractions of 30–60% on the TGA curves, shifted up to the higher fractions with increased oxygen pressure, and occurred as separated peaks B and B′ on the DTA–MS curves at 460–480 °C. The transformation of anatase to rutile occurred at 52% fraction (Fig. 4d), just after the grains had obviously cracked along the edges (Fig. 5a). The cracks may be correlated with the formation and increase in content of a rutile phase. Thus, it is apparent that the formation of rutile is involved in stage III.

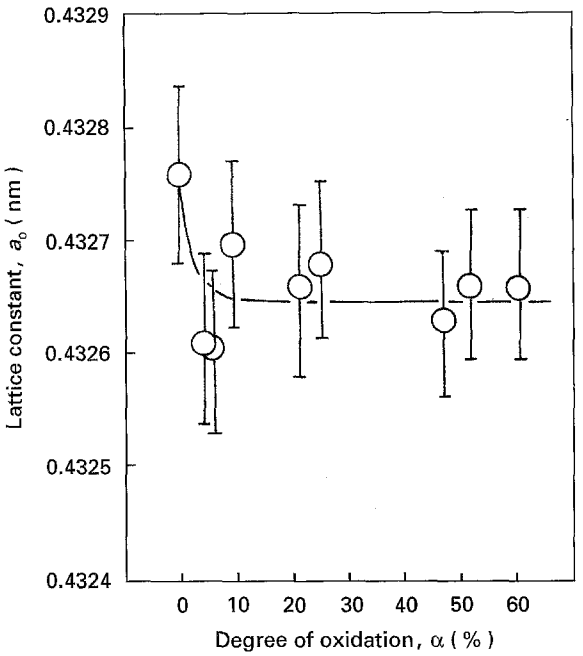

Figure 7 The lattice constant, a_0, of the sample oxidized at various degrees (oxygen pressure 10 kPa).

Comparison of the whole exothermic peak area obtained at each pressure showed that the area was little changed with oxygen pressure, suggesting that the exothermic peak contained no excess heat evolution due to the crystallization of anatase, as reported previously.

In stage IV, oxidation proceeded with constant evolution of heat and CO_2 gas with temperature. In contrast to a slight increase of the anatase phase, the rutile phase increased with the α fraction (Fig. 4), suggesting that as soon as a certain amount of the anatase was formed, the anatase transformed to rutile, the amount of the new phase being kept constant. During the transformation, the grains significantly cracked along the edges (Fig. 5b) and were eventually broken into pieces or flakes. Stage IV reflects such oxidation behaviour involving the continuous formation of anatase, followed by its transformation to rutile.

When the sample amount was decreased from 10.3 to 2.7 mg at the oxygen pressure of 10 kPa, the sharp peaks A/B and A′/B′ on the DTA curve changed to overlapping or combined peaks. This indicates that oxidation in stages II and III is influenced by the amount of sample, as well as by oxygen pressure. It is thought that the 10.3 mg sample, having a bed height of about 0.5 mm, cannot release quickly the heat generated by oxidation, resulting in a self-heating condition. As a result, whether two sharp peaks, or an overlapping or combined peak appear depends on both the sample amount and the oxygen pressure (Fig. 7).

5. Conclusions

Oxidation of a TiC powdered sample under non-isothermal conditions was carried out in a temperature range of 300–900 °C and at an oxygen pressure of 2–60 kPa, using a simultaneous TGA–DTA–MS apparatus. The results are summarized as follows.

Oxidation was divided into four stages, I–IV in an α fraction range of 0–20, 20–60 (stages II and III) and $> 60\%$. It was assumed that stage I was due to the formation of oxycarbide, TiC_xO_{1-x} ($0 < 1 - x < 0.5$), with slight evolution of heat and CO_2 gas. Oxidation in stage II, which correlated with the formation of anatase, was accelerated by oxygen pressures higher than 15 kPa, producing a sharp exothermic and CO_2 evolution peaks. Oxidation proceeded with gradual evolution of heat and CO_2 in stage III, in which a rutile phase was formed and increased in content with increasing temperature. It was noticed that the heat and CO_2 gas evolution behaviours were very similar throughout the period of oxidation. The sample amount also exerted a similar effect on oxidation to that of the oxygen pressure.

References

1. N. F. MACDONALD and C. E. RANSLEY, *Powder Metall* **3** (1959) 172.
2. M. REICHLE and J. J. NICKL, *J. Less-Common Metals* **27** (1972) 213.
3. Y. A. LAVRENKO, L. A. GLEBOV, A. P. POMITKIN, V. G. CHUPRINA and T. G. PROTSENKO. *Oxid. Metals* **9** (1975) 171.
4. R. W. STEWART and I. B. CUTLER, *J. Amer. Ceram. Soc.* **50** (1967) 176.
5. B. O. HAGLUND and B. LEHTINEN, in "Thermal Analysis". Proceeding of the Third ICTA (Davos, 1971) Vol. 3, p. 545. Ed by H. G. Wiedemann (Zurich, Switzerland)
6. D. K. CHATTERJEE and H. A. LIPSITT, *Metall. Trans.* **13A** (1982) 1837.
7. S. SHIMADA and M. KOZEKI, *J. Mater. Sci.* **27** (1992) 1869.
8. S. SHIMADA and T. ISHII, *J. Amer. Ceram. Soc.* **73** (1990) 2084.
9. S. SHIMADA, M. NISHISAKO, M. INAGAKI and K. YAMAMOTO, *ibid.* **98** (1995) 41.
10. S. SHIMADA, M. INAGAKI and T. MATSUI, *ibid.* **75** (1992) 2671.
11. S. SHIMADA and M. INAGAKI, *Solid State Ionics* 63–65 (1993) 312.
12. S. SHIMADA, *Oxid. Metals* **42** (1994) 357.

Received 8 September 1994
and accepted 7 June 1995